

Galactic Rotation Curve and Spiral Density Wave Parameters from 73 Masers

V.V. Bobylev^{1,2}, and A.T. Bajkova¹

¹*Pulkovo Astronomical Observatory, St. Petersburg, Russia*

²*Sobolev Astronomical Institute, St. Petersburg State University, Russia*

Abstract—Based on kinematic data on masers with known trigonometric parallaxes and measurements of the velocities of HI clouds at tangential points in the inner Galaxy, we have refined the parameters of the Allen-Santillan model Galactic potential and constructed the Galactic rotation curve in a wide range of Galactocentric distances, from 0 to 20 kpc. The circular rotation velocity of the Sun for the adopted Galactocentric distance $R_0 = 8$ kpc is $V_0 = 239 \pm 16$ km s⁻¹. We have obtained the series of residual tangential, ΔV_θ , and radial, ΔV_R , velocities for 73 masers. Based on these series, we have determined the parameters of the Galactic spiral density wave satisfying the linear Lin-Shu model using the method of periodogram analysis that we proposed previously. The tangential and radial perturbation amplitudes are $f_\theta = 7.0 \pm 1.2$ km s⁻¹ and $f_R = 7.8 \pm 0.7$ km s⁻¹, respectively, the perturbation wavelength is $\lambda = 2.3 \pm 0.4$ kpc, and the pitch angle of the spiral pattern in a two-armed model is $i = -5.2^\circ \pm 0.7^\circ$. The phase of the Sun χ_\odot in the spiral density wave is $-50^\circ \pm 15^\circ$ and $-160^\circ \pm 15^\circ$ from the residual tangential and radial velocities, respectively.

INTRODUCTION

A spectral (periodogram) analysis of the residual space velocities for various young Galactic objects (hydrogen clouds, OB stars, open star clusters, masers) tracing the spiral arms was used, for example, by Clemens (1985), Bobylev et al. (2008), and Bobylev and Bajkova (2010). In accordance with the model by Lin and Shu (1964), such spiral density wave parameters as the pitch angle, the perturbation amplitude and wavelength, and the phase of the Sun in the spiral density wave were determined.

Bajkova and Bobylev (2012) studied the space velocities of 44 masers from the range of Galactocentric distances 3–14 kpc. An amplitude of the velocity perturbations produced by the density wave differing significantly from zero was found only in the Galactocentric radial velocities of these sources, $f_R = 7.7 \pm 1.6$ km s⁻¹. In contrast, the amplitude of the velocity perturbations in the residual rotation velocities f_θ turned out to be close to zero, which looks strange. For example, the residual rotation velocities of hydrogen clouds and Cepheids show an amplitude of periodic perturbations $f_\theta \approx 6 \pm 1.5$ km s⁻¹ (Clemens 1985) and $f_\theta = 3.3 \pm 0.5$ km s⁻¹ (Bobylev and Bajkova 2012), respectively. Theoretical estimates also suggest that f_θ should not differ greatly from f_R (Burton 1971).

At present, there are data on about 80 Galactic masers that are distributed in the range of Galactocentric distances 0–20 kpc; the number of measured parallaxes constantly

increases. Determining consistent spiral density wave parameters obtained from both radial and tangential velocities is of great interest. This requires constructing a smooth rotation curve in a wide range of distances maximally close to the data. A wide variety of methods for determining a smooth rotation curve are known: constructing a composite curve from the rotation velocities using polynomials of various orders (Clemens 1985), solving Bottlinger’s kinematic equations using several terms of the Taylor expansion of the angular velocity of Galactic rotation (Zabolotskikh et al. 2002; Popova and Loktin 2005; Bobylev et al. 2008), approximating the rotation velocities by a set of exponential functions (Amôres et al. 2009).

Here, we apply the dynamical method. It consists in constructing the Galactic potential function. This approach is implemented, for example, in the three-component model Galactic potential (Allen and Santillan 1991; Khoperskov et al. 2013; Irrgang et al. 2013).

The goal of this paper is to refine the parameters of the three-component model Galactic potential described by Allen and Santillan (1991), to construct a smooth Galactic rotation curve in the range 0–20 kpc, and, on this basis, to determine the spiral density wave parameters from the residual tangential and radial velocities of the maximum number of masers with accurately measured trigonometric parallaxes known to date. To refine the parameters of the Galactic potential and to construct the rotation curve in a wide range of Galactocentric distances, 0–20 kpc, we use both data on masers with Galactocentric distances from the range 3–20 kpc and data on neutral hydrogen clouds at tangential points in the inner Galaxy ($R < 2$ kpc), where there are no reliable maser velocity measurements at present.

DATA

We use the maser coordinates, proper motions, and trigonometric parallaxes measured by VLBI with an error, on average, less than 10%. These masers are associated with very young objects, protostars of mostly high masses (but there are also low-mass ones; a number of massive supergiants are also known) located in regions of active star formation, and, thus, trace well the spiral arms.

One of the projects to obtain such data is the Japanese VERA (VLBI Exploration of Radio Astrometry) project aimed at the observations of Galactic H₂O masers at 22 GHz (Hirota et al. 2007) and SiO masers (there are very few such sources among young objects) at 43 GHz (Kim et al. 2008). Methanol (CH₃OH) masers are observed at 12 GHz in the USA on VLBA (Reid et al. 2009a). The observations of masers are also being carried out within the framework of the European VLBI network, which now includes three Russian stations of the QUASAR system (Rygl et al. 2010). The VLBI observations of radio stars in continuum at 8.4 GHz are being carried out with the same goals (Dzib et al. 2011).

Complete information about 44 masers (coordinates, line-of-sight velocities, proper motions, and parallaxes) is presented in Bajkova and Bobylev (2012). Subsequently, a number of papers with new measurements have been published. New data on 31 sources are presented in Table 1. Note that nine of them have no maser emission, but they are fairly bright radio stars for which the parallaxes were measured by VLBI with a high accuracy in continuum. These include several low-mass stars in Taurus (Hubble 4, V773

Tau AB, T Tau N, HDE 283572, and HP Tau/G2), Serpens (EC 95), and Ophiuchus (S1 and DoAr21 Oph) as well as the high-mass Xray binary Cyg X-1 with one of its components being a black hole.

In the inner Galaxy ($R < 2$) kpc, as yet there are virtually now data on masers. The trigonometric parallaxes (Reid et al. 2009b) were measured only for two maser spots in the Sgr B2 region. However, we do not use them for our studies and provide them only for the purposes of illustration, because the spiral pattern of the Galaxy begins from the bar ends ($R > 3$ kpc). Therefore, our final sample of sources based on which the spiral density wave parameters are determined contains only 73 sources.

As a rule, invoking data on objects of various classes is required to refine the parameters of the model Galactic potential and to construct the rotation curve in a wide range of distances. For example, apart from data on 30 masers, Irrgang et al. (2013) used both data on hydrogen in the inner Galaxy ($R < 2$ kpc) from Burton and Gordon (1978) and data on CO in the middle Galactic region in the range of distances 3–8 kpc from Clemens (1985) to construct the Galactic potential. This was done because of the large “gap” in the distribution of masers. In our case, the situation is distinctly different: we have already 73 masers that fill the range of distances 3–14 kpc fairly densely; therefore, we use only the line-of-sight velocities of neutral hydrogen clouds located at tangential points in the inner Galaxy (Burton and Gordon 1978).

METHODS AND APPROACHES

The values of two quantities should be known to determine the circular velocities of stars: the Galactocentric distance of the Sun R_0 , which we take to be 8 kpc, and the circular rotation velocity of the solar neighborhood V_0 .

Determining the Velocity V_0

To determine the velocity $V_0 = R_0|\Omega_0|$ from observational data, we use the equations derived from Bottlinger’s formulas with the angular velocity of Galactic rotation Ω expanded in a series to terms of the second order of smallness in r/R_0 :

$$V_r = -u_\odot \cos b \cos l - v_\odot \cos b \sin l - w_\odot \sin b + R_0(R - R_0) \sin l \cos b \Omega'_0 + 0.5R_0(R - R_0)^2 \sin l \cos b \Omega''_0, \quad (1)$$

$$V_l = u_\odot \sin l - v_\odot \cos l + (R - R_0)(R_0 \cos l - r \cos b) \Omega'_0 + (R - R_0)^2(R_0 \cos l - r \cos b) 0.5 \Omega''_0 - r \Omega_0 \cos b, \quad (2)$$

$$V_b = u_\odot \cos l \sin b + v_\odot \sin l \sin b - w_\odot \cos b - R_0(R - R_0) \sin l \sin b \Omega'_0 - 0.5R_0(R - R_0)^2 \sin l \sin b \Omega''_0, \quad (3)$$

where V_r is the line-of-sight velocity of the star (in km s^{-1}); $r = 1/\pi$ is the heliocentric distance of the star; $V_l = 4.74r\mu_l \cos b$ and $V_b = 4.74r\mu_b$ are the proper motion velocity components of the star (in mas yr^{-1}) in the l and b directions, respectively; the coefficient 4.74 is the quotient of the number of kilometers in an astronomical unit by the number of seconds in a tropical year; $u_\odot, v_\odot, w_\odot$ are the stellar group velocity components relative

Table 1: Initial data on the sources

Source	α	δ	$\pi(\sigma_\pi)$	$\mu_\alpha^*(\sigma_{\mu_\alpha})$	$\mu_\delta(\sigma_{\mu_\delta})$	$V_r(\sigma_{V_r})$	Ref
IRAS 5168+36	80.0920	36.6324	.532(.053)	.23(1.07)	-3.14(.28)	-15.5(1.9)	(1)
NML Cyg	311.6064	40.1165	.620(.047)	-1.55(.42)	-4.59(.41)	-.1(2)	(2)
IRAS20143+36	304.0467	36.7167	.368(.037)	-2.99(.16)	-4.37(.43)	7.0(3)	(3)
PZ Cas	356.0137	61.7895	.390(.022)	-3.20(.10)	-2.50(.10)	-36.1(.7)	(4)
IRAS22480+60	342.4953	60.2991	.400(.025)	-2.58(.33)	-1.91(.17)	-50.8(3.5)	(5)
RCW 122	260.0242	-38.9603	.296(.026)	-.73(.04)	-2.83(.50)	-12.6(5)	(6)
Hubble 4	64.6960	28.3354	7.530(.030)	4.30(.05)	-28.90(.30)	6.1(1.7)	(7)
HDE 283572	65.4952	28.3018	7.780(.040)	8.88(.06)	-26.60(.10)	6.0(1.5)	(7)
T Tau N	65.4976	19.5351	6.820(.030)	12.35(.04)	-12.80(.05)	7.7(1.2)	(8)
V773 Tau AB	63.5538	28.2034	7.700(.190)	8.30(.50)	-23.60(.50)	7.5(.5)	(9)
HP Tau/G2	68.9757	22.9037	6.200(.030)	13.85(.03)	-15.40(.20)	6.8(1.8)	(10)
S1 Oph	246.6424	-24.3912	8.550(.500)	-3.88(.69)	-31.55(.50)	3.0(3)	(11)
DoAr21 Oph	246.5126	-24.3934	8.200(.370)	-26.47(.92)	-28.23(.73)	3.0(3)	(11)
EC 95	277.4912	1.2128	2.410(.020)	.70(.02)	-3.64(.10)	9.0(3)	(12)
G074.03-1.71	306.2796	34.8327	.629(.017)	-3.79(.18)	-4.88(.25)	13.4(3)	(13)
G075.76+0.33	305.4212	37.4248	.285(.022)	-3.08(.06)	-4.56(.08)	-9.6(3)	(13)
G075.78+0.34	305.4334	37.4437	.281(.034)	-2.79(.07)	-4.72(.07)	3.4(3)	(13)
G076.38-0.61	306.8562	37.3801	.770(.053)	-3.73(3.00)	-3.84(3.0)	6.9(3)	(13)
G079.87+1.17	307.6214	41.2649	.620(.027)	-3.23(1.31)	-5.19(1.31)	-4.6(3)	(13)
G090.21+2.32	315.5946	50.0523	1.483(.038)	-.67(3.13)	-.90(3.13)	-6.2(3)	(13)
G092.67+3.07	317.3405	52.3770	.613(.020)	-.69(.26)	-2.25(.33)	-3.7(3)	(13)
G105.41+9.87	325.7769	66.1153	1.129(.063)	-.21(2.38)	-5.49(2.38)	-12.1(3)	(13)
IRAS20126+41	303.6084	41.2257	.610(.020)	-4.14(.13)	-4.14(.13)	-4.0(5)	(14)
W33 A f1	273.6435	-17.8644	.408(.025)	.19(.08)	-2.52(.32)	34.9(5)	(15)
W33 A f2	273.6649	-17.8668	.396(.032)	-.36(.08)	-2.22(.13)	37.0(5)	(15)
W33 Main f2	273.5576	-17.9225	.343(.037)	-.60(.11)	-.99(.13)	34.1(5)	(15)
G012.88+0.48	272.9646	-17.5247	.340(.036)	.12(.13)	-2.66(.23)	29.4(5)	(15)
IRAS05137+39	79.3073	39.3722	.086(.027)	.30(.10)	-.89(.27)	-26.0(3)	(16)
Cyg X-1	299.5903	35.2016	.539(.033)	-3.78(.06)	-6.40(.12)	15.5(5)	(17)
SgrB2N	266.8330	-28.3720	.128(.015)	-.32(.05)	-4.69(.11)	64.0(5)	(18)
SgrB2M	266.8340	-28.3845	.130(.012)	-1.23(.04)	-3.84(.11)	61.0(5)	(18)

Note. α and δ in deg., π in mas, $\mu_\alpha^* = \mu_\alpha \cos \delta$ and μ_δ in mas/yr, $V_r = V_r(LSR)$ in km/s, The numbers mark the references to papers: (1) Sakai et al. (2012); (2) Zhang et al. (2012); (3) Yamaguchi et al. (2012); (4) Kusuno et al. (2012); (5) Imai et al. (2012); (6) Wu et al. (2012); (7) Torres et al. (2007); (8) Loinard et al. (2007); (9) Lestrade et al. (1999); (10) Torres et al. (2009); (11) Loinard et al. (2008); (12) Dzib et al. (2010); (13) Xu et al. (2013); (14) Moscadelli et al. (2011); (15) Immer et al. (2013); (16) Honma et al. (2011); (17) Reid et al. (2011); (18) Reid et al. (2009b).

to the Sun taken with the opposite sign (the velocity U is directed toward the Galactic center, V is in the direction of Galactic rotation, W is directed to the north Galactic pole); R_0 is the Galactocentric distance of the Sun; Ω_0 is the angular velocity of rotation at the distance R_0 ; the parameters Ω'_0 and Ω''_0 are the first and second derivatives of the angular velocity, respectively; the distance of the star to the Galactic rotation axis R is calculated from the formula

$$R^2 = r^2 \cos^2 b - 2R_0 r \cos b \cos l + R_0^2. \quad (4)$$

Equations (1) are solved by the least-squares method with weights of the form

$$w_r = S_0 / \sqrt{S_0^2 + \sigma_{V_r}^2}, \quad w_l = \beta^2 S_0 / \sqrt{S_0^2 + \sigma_{V_l}^2}, \quad w_b = \gamma^2 S_0 / \sqrt{S_0^2 + \sigma_{V_b}^2}, \quad (5)$$

where S_0 is the ‘‘cosmic’’ dispersion taken to be 8 km s^{-1} ; σ_{V_r} , σ_{V_l} , and σ_{V_b} are the errors in the corresponding observed velocities; $\beta = \sigma_{V_r} / \sigma_{V_l}$ and $\gamma = \sigma_{V_r} / \sigma_{V_b}$ are the scale factors that we determined using data on open star clusters (Bobylev et al. 2007), $\beta = 1$ and $\gamma = 2$.

Determining the Radial and Tangential Velocities

For hydrogen clouds, there is only the line-of-sight velocity V_r . The projection of the circular rotation velocity V_θ is calculated from the well-known formula (Burton 1971)

$$V_\theta = |R\Omega_0| + RV_r / (R_0 \sin l \cos b). \quad (6)$$

Note that radio astronomers usually give the line-of-sight velocities relative to the local standard of rest (this is true for both masers and the line-of-sight velocities of HI clouds). Therefore, they should be reduced to the heliocentric frame of reference (in Table 1, the line-of-sight velocities of all stars are given relative to the local standard of rest, LSR). This requires using the parameters of the standard solar motion

$$\begin{aligned} (\alpha, \delta)_{1900} &= (270^\circ, 30^\circ), \quad V = 20 \text{ km s}^{-1}, \\ (U, V, W)_{LSR} &= (10.3, 15.3, 7.7) \text{ km s}^{-1}. \end{aligned} \quad (7)$$

Since the hydrogen clouds are assumed to be located at tangential points (in the first or fourth quadrants), the following simple relations hold for them:

$$\begin{aligned} R &= R_0 |\sin l|, \\ r &= R_0 \cos l. \end{aligned} \quad (8)$$

The spatial coordinates of all objects are calculated in a rectangular X, Y, Z coordinate system. The components of the observed space velocities U and V are calculated from the projections V_r , V_l , and V_b ; these are used to find two projections: V_R directed radially away from the Galactic center and V_θ orthogonal to it:

$$\begin{aligned} V_R &= -U \cos \theta + (V_0 + V) \sin \theta, \\ V_\theta &= U \sin \theta + (V_0 + V) \cos \theta, \end{aligned} \quad (9)$$

where the object’s position angle θ is defined as $\tan \theta = Y / (R_0 - X)$. The velocities U and V are assumed to be free from the solar velocity relative to the centroid $V_\odot(u_\odot, v_\odot, w_\odot)$.

The Model Galactic Potential

Here, we use the model Galactic potential by Allen and Santillan (1991). The axisymmetric Galactic potential is represented as the sum of three components—the central (bulge), disk, and halo ones:

$$\Phi = \Phi_C + \Phi_D + \Phi_H. \quad (10)$$

The central component of the Galactic potential in cylindrical coordinates (r, θ, z) is represented in the form proposed by Miyamoto and Nagai (1975):

$$\Phi_C = -\frac{M_C}{(r^2 + z^2 + b_C^2)^{1/2}}, \quad (11)$$

where M_C is the mass, b_C is the scale length. The disk component is represented as the Miyamoto–Nagai (1975) disk:

$$\Phi_D = -\frac{M_D}{\{r^2 + [a_D + (z^2 + b_D^2)^{1/2}]^2\}^{1/2}}, \quad (12)$$

where M_D is the mass, a_D , and b_D are the scale lengths. The halo component is represented in the form proposed by Allen and Martos (1986):

$$\Phi_H = -\frac{M(R)}{R} - \int_R^{100} \frac{1}{R'} \frac{dM(R')}{dR'} dR', \quad (13)$$

where

$$M(R) = \frac{M_H(R/a_H)^{2.02}}{1 + (R/a_H)^{1.02}},$$

where M_H is the mass, a_H is the scale length. If R is measured in kpc and M_C, M_D, M_H are measured in units of the Galactic mass (M_G), $2.32 \times 10^7 M_\odot$, then the gravitational constant $G = 1$ and the unit of measurement for the potential Φ and its individual components (2)–(4) is $100 \text{ km}^2 \text{ s}^{-2}$.

The Rotation Curve

The tangential velocities are expressed in terms of the Galactic potential components as

$$V_\theta^2 = R \left\{ \frac{\partial \Phi_C}{\partial R} + \frac{\partial \Phi_D}{\partial R} + \frac{\partial \Phi_H}{\partial R} \right\}, \quad (14)$$

Substituting Eqs. (2)–(4) into (5) and setting $z = 0$, we will obtain an analytical expression for the smooth rotation curve:

$$V_\theta = \left\{ \frac{R^2 M_C}{(R^2 + b_C^2)^{3/2}} + \frac{R^2 M_D}{(R^2 + (a_D + b_D)^2)^{3/2}} + \frac{R^{1.02} M_H}{a_H^{2.02} (1 + (R/a_H)^{1.02})} \right\}^{1/2}. \quad (15)$$

The parameters of the model potential are determined by least-squares fitting to the measured velocities of the masers and hydrogen clouds. The residual tangential velocities ΔV_θ used below to determine the spiral density wave parameters are found as the differences of the tangential velocities V_θ and the smooth rotation curve (6).

Estimating the Spiral Density Wave Parameters

To take into account the influence of the spiral density wave, we used the simplest kinematic model based on the linear density wave theory by Lin and Shu (1964), in which the potential perturbation is in the form of a traveling wave. Then,

$$\begin{aligned} V_R &= -f_R \cos \chi, \\ \Delta V_\theta &= f_\theta \sin \chi, \end{aligned} \quad (16)$$

Here, V_R and ΔV_θ are the radial and tangential velocity perturbations produced by the spiral density wave, f_R and f_θ are the amplitudes of the radial and tangential velocity perturbations, i is the spiral pitch angle ($i < 0$ for winding spirals), m is the number of arms (here, we take $m = 2$), the wave phase χ is

$$\chi = m[\cot(i) \ln(R/R_0) - \theta] + \chi_\odot, \quad (17)$$

where χ_\odot is the radial phase of the Sun in the spiral density wave; we measure this angle (following Rohlfs 1977) from the center of the Carina–Sagittarius spiral arm ($R \approx 7$ kpc).

The parameter λ , the distance (along the Galactocentric radial direction) between adjacent spiral arm segments in the solar neighborhood (the wavelength of the spiral density wave), is calculated from the relation

$$\frac{2\pi R_0}{\lambda} = m \cot(i). \quad (18)$$

Let there be a series of measured velocities $V_n(R_n)$ (these can be both radial, V_R , and residual tangential, ΔV_θ , velocities) at points with Galactocentric distances R_n and position angles θ_n , $n = 1, \dots, N$ where N is the number of objects. The objective of our spectral analysis is to extract a periodicity from the data series in accordance with the model (7)–(9) describing a spiral density wave with parameters $f_R(f_\theta)$, $\lambda(i)$, and χ_\odot .

Having taken into account the logarithmic character of the spiral density wave and the position angles of the objects θ_n , our spectral (periodogram) analysis of the series of velocity perturbations is reduced to calculating the square of the amplitude (power spectrum) of the standard Fourier transform (Bajkova and Bobylev 2012):

$$\bar{V}_{\lambda_k} = \frac{1}{N} \sum_{n=1}^N V'_n(R'_n) \exp\left(-j \frac{2\pi R'_n}{\lambda_k}\right), \quad (19)$$

where \bar{V}_{λ_k} is the k th harmonic of the Fourier transform, with the wavelength being $\lambda_k = D/k$, D is the period of the series being analyzed,

$$R'_n = R_0 \ln(R_n/R_0), \quad (20)$$

$$V'_n(R'_n) = V_n(R_n) \times \exp(jm\theta_n).$$

The algorithm of searching for periodicities modified to properly determine not only the wavelength but also the amplitude of the perturbations is described in detail in Bajkova and Bobylev (2012).

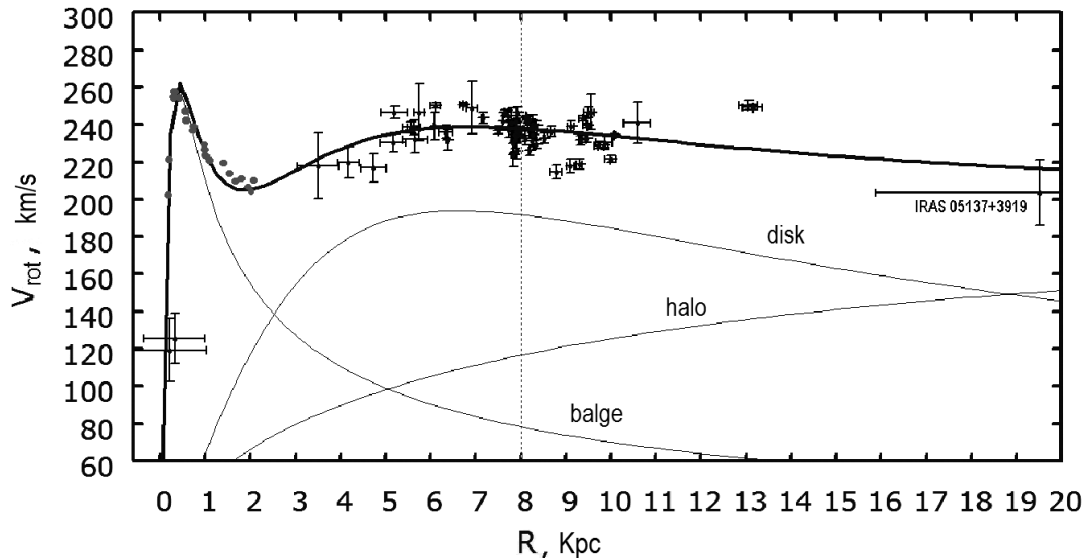


Figure 1: Galactic rotation curve (thick line), the thin lines indicate the contribution from the bulge, disk, and halo to the rotation curve, the dotted line marks the position of the Sun, the gray circles indicate the data on neutron hydrogen (Burton and Gordon 1978), the dots with error bars indicate the data on masers.

Obviously, the sought-for wavelength λ corresponds to the peak value of the power spectrum S_{peak} . The pitch angle of the spiral density wave can be derived from Eq. (9). We determine the perturbation amplitude and phase by fitting the harmonic with the wavelength found to the observational data. The following relation can also be used to estimate the perturbation amplitude:

$$f_R(f_\theta) = \sqrt{4 \times S_{peak}}.$$

RESULTS

The Velocity V_0

We obtained several solutions of the system of equations (1) by the least-squares method with various constraints on the sample radius (r) and the parallax error (e_π/π). These solutions differ insignificantly, but it should be noted that Ω_0 increases with decreasing sample radius from $\Omega_0 = 28 \text{ km s}^{-1} \text{ kpc}^{-1}$ for all masers to $\Omega_0 = 32 \text{ km s}^{-1} \text{ kpc}^{-1}$ for the nearest ones.

For example, based on the entire sample of masers, we obtained the following solution:

$$\begin{aligned} (u_\odot, v_\odot, w_\odot) &= (7.4, 16.3, 8.3) \pm (1.2, 1.1, 1.0) \text{ km s}^{-1}, \\ \Omega_0 &= 28.7 \pm 0.6 \text{ km s}^{-1} \text{ kpc}^{-1}, \\ \Omega'_0 &= -4.11 \pm 0.13 \text{ km s}^{-1} \text{ kpc}^{-2}, \\ \Omega''_0 &= 0.676 \pm 0.057 \text{ km s}^{-1} \text{ kpc}^{-3}, \end{aligned} \tag{21}$$

Table 2: Parameters of the model Galactic potential

M_C	493 M_G
M_D	4599 M_G
M_H	6526 M_G
b_C	0.2815 kpc
a_D	4.4555 kpc
b_D	0.25 kpc
a_H	15.9 kpc

with the error per unit weight being $\sigma_0 = 8.11 \text{ km s}^{-1}$.

Based on a sample of 55 masers from the range $r < 3.5 \text{ kpc}$ with $e_\pi/\pi < 10\%$, we obtained the following solution:

$$(u_\odot, v_\odot, w_\odot) = (8.8, 17.3, 7.9) \pm (1.4, 1.3, 1.0) \text{ km s}^{-1}, \quad (22)$$

$$\begin{aligned} \Omega_0 &= 29.9 \pm 1.1 \text{ km s}^{-1} \text{ kpc}^{-1}, \\ \Omega'_0 &= -4.27 \pm 0.20 \text{ km s}^{-1} \text{ kpc}^{-2}, \\ \Omega''_0 &= 0.915 \pm 0.166 \text{ km s}^{-1} \text{ kpc}^{-3}. \end{aligned} \quad (23)$$

In this case, the error per unit weight is $\sigma_0 = 7.65 \text{ km s}^{-1}$, which is considerably smaller than that in the previous case. Therefore, we adopted the solution for Ω_0 obtained from 55 masers with more accurate parallaxes. Since Ω_0 is a local parameter, the solution obtained from nearer objects with more accurate parallaxes may be considered to be more correct than that obtained from all objects, including the distant ones. The sought-for circular velocity of the Sun will then be $V_0 = R_0|\Omega_0| = 239 \pm 16 \text{ km s}^{-1}$.

The rotation velocities (V_θ) of the hydrogen clouds and masers calculated with the velocity V_0 found are presented in Fig. 1. We took into account the group motion of the stars relative to the Sun (11). It can be seen that the velocities (11), especially v_\odot , differ from the LSR parameters $(U_\odot, V_\odot, W_\odot)_{LSR} = (11.1, 12.2, 7.3) \text{ km s}^{-1}$ found by Schönrich et al. (2010). In our opinion (Bobylev and Bajkova 2010), such a difference is due to the influence of the spiral density wave. Based on a sample of 30 masers from the Orion arm, Xu et al. (2013) found a difference $\Delta v_\odot \approx 5 \text{ km s}^{-1}$ compared to the velocity from Schönrich et al. (2010).

Note that the Galactic rotation curve constructed with the parameters (12) is applicable only in a limited solar neighborhood with a radius of 4–6 kpc and goes upward at large $R > 14 \text{ kpc}$ (Bobylev and Bajkova 2010). In such an approach, for example, the residual velocity of the maser IRAS 05137+3919 will be very high. Thus, the rotation curve is currently difficult to construct by expanding the angular velocity (1) into a series because of the very small amount of data at large distances R . Therefore, here we use an approach based on a refinement of the Galactic potential parameters to construct the rotation curve.

The Galactic Potential and Rotation Curve

The refined parameters of the model Galactic potential found by fitting Eq. (5) (by the least-squares method) to the measured velocities of the masers and hydrogen clouds are given in Table 2. The Galactic rotation curve and the contributions from each of the three potential components to the total velocity obtained from Eq. (6) are shown in Fig. 1. The masses M_C , M_D , and M_H from Table 2 were multiplied by 100.

The Spiral Density Wave Parameters

In Fig. 2, the radial velocities V_R of the masers and their residual rotation velocities ΔV_θ are plotted against the distance R' (Eq. (10)), and Fig. 3 shows their power spectra. The significance level of the main peak is 0.999 for the radial velocities (Fig. 3a) and 0.86 for the rotation velocities (Fig. 3b). As a result, we obtained the following spiral density wave parameters based on our sample of 73 masers independently for each of the velocity components (V_R and ΔV_θ):

$$\begin{aligned}
 f_R &= 7.8 \pm 0.7 \text{ km s}^{-1}, \\
 f_\theta &= 7.0 \pm 1.2 \text{ km s}^{-1}, \\
 \lambda_R &= 2.4 \pm 0.4 \text{ kpc}, \\
 \lambda_\theta &= 2.3 \pm 0.4 \text{ kpc}, \\
 (\chi_\odot)_R &= -160^\circ \pm 15^\circ, \\
 (\chi_\odot)_\theta &= -50^\circ \pm 15^\circ.
 \end{aligned}
 \tag{24}$$

The pitch angle for the model of a two-armed pattern is $i = -5.2^\circ \pm 0.7^\circ$.

DISCUSSION

Parameters of the Galactic Rotation Curve

Based on 52 Galactic masers, Honma et al. (2012) found the angular velocity of Galactic rotation $\Omega_0 = 31.09 \pm 0.78 \text{ km s}^{-1} \text{ kpc}^{-1}$ and the linear velocity $V_0 = R_0 |\Omega_0| = 238 \pm 14 \text{ km s}^{-1}$ (at $R_0 = 8.05 \pm 0.45 \text{ kpc}$ found). The parameters (12) are in good agreement with these results. Therefore, it should be noted that the masers belong to the most rapidly rotating fraction of the Galactic disk. This is not surprising, because they are the youngest objects that have recently been formed from hydrogen.

Other authors found a high angular velocity of their Galactic rotation even from a smaller number of masers. Based on a sample of 18 masers, Reid et al. (2009a) found $\Omega_0 = 30.3 \pm 0.9 \text{ km s}^{-1} \text{ kpc}^{-1}$. Based on the same sample, McMillan and Binney (2010) showed that Ω_0 lies within the range $29.9\text{--}31.6 \text{ km s}^{-1} \text{ kpc}^{-1}$ at various R_0 and obtained an estimate of $V_0 = 247 \pm 19 \text{ km s}^{-1}$ for $R_0 = 7.8 \pm 0.4 \text{ kpc}$. Based on a sample of 18 masers, Bovy et al. (2009) found $V_0 = 244 \pm 13 \text{ km s}^{-1}$ for $R_0 = 8.2 \text{ kpc}$. Based on a sample of 18 masers, Brunthaler et al. (2011) found $V_0 = 246 \pm 7 \text{ km s}^{-1}$ and $R_0 = 8.3 \pm 0.23 \text{ kpc}$. Using 28 masers, Stepanishchev and Bobylev (2011) obtained an estimate of $V_0 = 243 \pm 16 \text{ km s}^{-1}$ ($R_0 = 8.0 \pm 0.5 \text{ kpc}$). The parameters of the Galactic rotation curve (12) found are in good agreement with the results of analyzing other young objects of the Galactic disk rapidly rotating around the center. For example, based on

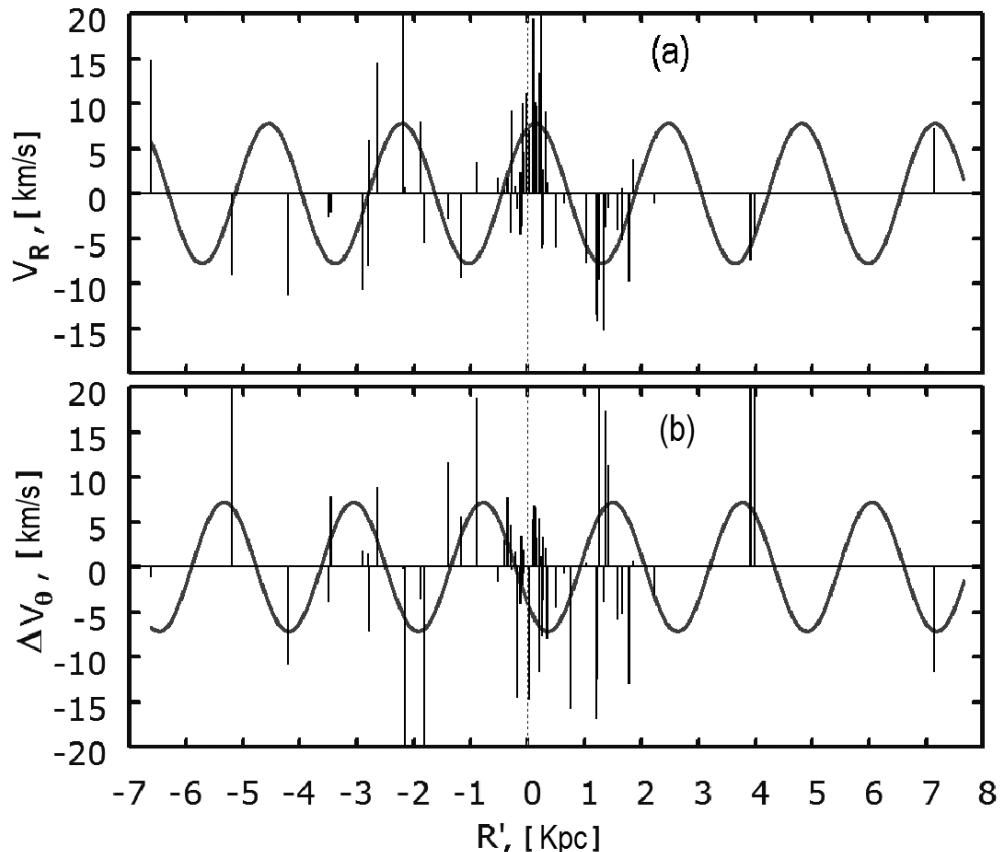


Figure 2: (a) Galactocentric radial velocities V_R of the masers versus distance R' ; (b) their residual rotation velocities ΔV_θ . The dotted line marks the position of the Sun.

OB associations, Mel'nik and Dambis (2009) found $\Omega_0 = 31 \pm 1 \text{ km s}^{-1} \text{ kpc}^{-1}$; based on a sample of blue supergiants, Zabolotskikh et al. (2002) obtained $\Omega_0 = 29.6 \pm 1.6 \text{ km s}^{-1} \text{ kpc}^{-1}$ and $\Omega'_0 = -4.76 \pm 0.32 \text{ km s}^{-1} \text{ kpc}^{-2}$; based on OB3 stars, Bobylev and Bajkova (2001) found $\Omega_0 = 31.5 \pm 0.9 \text{ km s}^{-1} \text{ kpc}^{-1}$, $\Omega'_0 = -4.49 \pm 0.12 \text{ km s}^{-1} \text{ kpc}^{-2}$ and $\Omega''_0 = 1.05 \pm 0.38 \text{ km s}^{-1} \text{ kpc}^{-3}$. Schönrich (2012) obtained an estimate of $V_0 = 250 \pm 9 \text{ km s}^{-1}$ for $R_0 = 8.27 \pm 0.29 \text{ kpc}$ from data on $\approx 220\,000$ stars from the SEGUE (Sloan Extension for Galactic Understanding and Exploration) catalogue.

The Galactic Potential

Irrgang et al. (2013) considered three model Galactic potentials constructed from data on hydrogen clouds and masers. In all cases, the velocity V_0 was found to be close to 240 km s^{-1} (for $R_0 \approx 8.3 \text{ kpc}$). The potentials differ by the expressions describing the halo contribution. In particular, model I, just as in our case, is a refinement of the model by Allen and Santillan (1991). Note that Irrgang et al. (2013) used both HI data at tangential points from Burton and Gordon (1978) and CO data from Clemens (1985). The rotation curve for model I from Irrgang et al. (2013) in the region 4.5 kpc passes closer to the CO observations above the masers, although, on the whole, the results turned

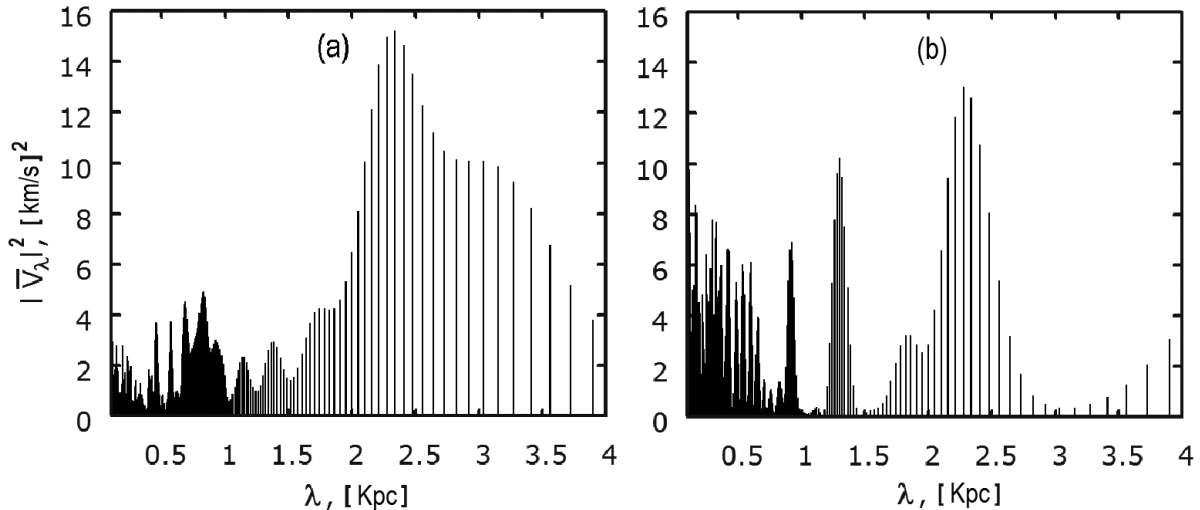


Figure 3: (a) Power spectrum for the radial velocities V_R of the masers; (b) power spectrum for their residual rotation velocities ΔV_θ .

out to be close. However, with regard to the approach of the rotation curve to the data on masers in the entire range, our curve (Fig. 1) fits better the data. This turned out to be important for analyzing the periodic perturbations produced by the influence of the spiral density wave.

Spiral Density Wave Parameters

Based on the radial (V_R) velocities of 44 masers, Bajkova and Bobylev (2012) obtained the following parameters related to the influence of the spiral density wave: the perturbation amplitude $f_R = 7.7_{-1.5}^{+1.7}$ km s $^{-1}$, the perturbation wavelength $\lambda = 2.2_{-0.1}^{+0.4}$ kpc, the pitch angle of the spiral density wave for the model of a two-armed pattern ($m = 2$) $i = -5_{-0.9}^{+0.2^\circ}$, and the Sun's phase in the spiral density wave $\chi_\odot = -147_{-17}^{+3^\circ}$. The parameters (13) are in good agreement with these results.

Here, for the first time we have found parameters of the perturbations produced by the spiral density wave in the residual rotation velocities (ΔV_θ) of masers that differ significantly from zero. Previously, it was possible to reveal such periodicities in the residual rotation velocities of hydrogen clouds (Clemens 1985) or middle-age Cepheids (Bobylev and Bajkova 2012). As can be seen from solution (13) and Fig. 2, the perturbation amplitude and wavelength found from both radial and tangential velocities are in good agreement between themselves. There is a significant discrepancy only in the Sun's phases, $\Delta\chi_\odot = 110^\circ$, in the spiral density wave. The value of χ_\odot obtained from the radial velocities is more trustworthy, because it agrees better with the position of the Sun in the spiral pattern that we found previously (Bobylev and Bajkova 2013) by an independent method from our analysis of the spatial distribution of masers, $\chi_\odot = -152^\circ$.

CONCLUSIONS

Based on kinematic data on 73 masers with known trigonometric parallaxes measured by VLBI and measurements of the velocities of HI clouds at tangential points in the inner Galaxy ($R < 2$ kpc), we refined the parameters of the Allen-Santillan (1991) model Galactic potential and, on this basis, constructed the Galactic rotation curve in a wide range of Galactocentric distances, from 0 to 20 kpc. The circular rotation velocity of the Sun for the adopted Galactocentric distance $R_0 = 8$ kpc was found to be $V_0 = 239 \pm 16$ km s⁻¹.

Based on the series of residual tangential, ΔV_θ , and radial, V_R , velocities for masers, we determined the parameters of the Galactic spiral density wave satisfying the linear Lin-Shu model using the method of periodogram analysis that we proposed previously. The tangential and radial perturbation amplitudes are $f_\theta = 7.0 \pm 1.2$ km s⁻¹ and $f_R = 7.8 \pm 0.7$ km s⁻¹, respectively, the perturbation wavelength is $\lambda = 2.3 \pm 0.4$ kpc, and the pitch angle of the spiral pattern in a two-armed model is $i = -5.2^\circ \pm 0.7^\circ$. The phase of the Sun χ_\odot in the spiral density wave is $-50^\circ \pm 15^\circ$ and $-160^\circ \pm 15^\circ$ from the residual tangential and radial velocities, respectively.

ACKNOWLEDGMENTS

We are grateful to the referee for helpful remarks that contributed to a improvement of the paper. This work was supported by the “Nonstationary Phenomena in Objects of the Universe” Program of the Presidium of the Russian Academy of Sciences and the “Multiwavelength Astrophysical Research” grant no. NSh-16245.2012.2 from the President of the Russian Federation. In our work, we widely used the SIMBAD astronomical database.

REFERENCES

1. C. Allen and M. A. Martos, *Rev. Mex. Astron. Astrofis.* 13, 137 (1986).
2. C. Allen and A. Santillan, *Rev. Mex. Astron. Astrofis.* 22, 255 (1991).
3. E.B. Amôres, J.R.D. Lépine, and Yu.N. Mishurov, *Mon. Not. R. Astron. Soc.* 400, 1768 (2009).
4. A.T. Bajkova and V.V. Bobylev, *Astron. Lett.* 38, 549 (2012).
5. V.V. Bobylev and A.T. Bajkova, *Mon. Not. R. Astron. Soc.* 408, 1788 (2010).
6. V.V. Bobylev and A.T. Bajkova, *Astron. Lett.* 37, 526 (2011).
7. V.V. Bobylev and A.T. Bajkova, *Astron. Lett.* 38, 638 (2012).
8. V.V. Bobylev and A.T. Bajkova, *Astron. Lett.* 39, 532 (2013).
9. V.V. Bobylev, A.T. Bajkova, and A. S. Stepanishchev, *Astron. Lett.* 34, 515 (2008).
10. J. Bovy, D.W. Hogg, and H.-W. Rix, *Astrophys. J.* 704, 1704 (2009).
11. A. Brunthaler, M.J. Reid, K.M. Menten, et al., *Astron. Nachr.* 332, 461 (2011).
12. W.B. Burton, *Astron. Astrophys.* 10, 76 (1971).
13. W.B. Burton and M. A. Gordon, *Astron. Astrophys.* 63, 7 (1978).
14. D.P. Clemens, *Astrophys. J.* 295, 422 (1985).
15. S. Dzib, L. Loinard, A.J. Mioduszewski, et al., *Astrophys. J.* 718, 610 (2010).
16. S. Dzib, L. Loinard, L.F. Rodriguez, et al., *Astrophys. J.* 733, 71 (2011).
17. T. Hirota, T. Bushimata, Y.K. Choi, et al., *Publ. Astron. Soc. Jpn.* 59, 897 (2007).

18. M. Honma, T. Hirota, Y. Kan-ya, et al., *Publ. Astron. Soc. Jpn.* 63, 17 (2011).
19. M. Honma, T. Nagayama, K. Ando, et al., *Publ. Astron. Soc. Jpn.* 64, 136 (2012).
20. H. Imai, N. Sakai, H. Nakanishi, et al., *Publ. Astron. Soc. Jpn.* 64, 142 (2012).
21. K. Immer, M.J. Reid, K.M. Menten, et al., *Astron. Astrophys.* 553, 1171 (2013).
22. A. Irrgang, B. Wilcox, E. Tucker, et al., *Astron. Astrophys.* 549, 137 (2013).
23. S.A. Khoperskov, E.O. Vasiliev, A.M. Sobolev, et al., *Mon. Not. R. Astron. Soc.* 428, 2311 (2013).
24. M.K. Kim, T. Hirota, M. Honma, et al., *Publ. Astron. Soc. Jpn.* 60, 991 (2008).
25. K. Kusuno, A. Yoshiharu, I. Hiroshi, et al., in *Proceedings of the East Asia VLBI Workshop 2012, May 30–Jun. 2, 2012* (2012).
26. J.-F. Lestrade, R.A. Preston, D.L. Jones, et al., *Astron. Astrophys.* 344, 1014 (1999).
27. C.C. Lin and F.H. Shu, *Astrophys. J.* 140, 646 (1964).
28. L. Loinard, R.M. Torres, A.J. Mioduszewski, et al., *Astrophys. J.* 671, 546 (2007).
29. L. Loinard, R.M. Torres, A.J. Mioduszewski, et al., *Astrophys. J.* 671, L29 (2008).
30. P.J. McMillan and J.J. Binney, *Mon. Not. R. Astron. Soc.* 402, 934 (2010).
31. A.M. Mel'nik and A.K. Dambis, *Mon. Not. R. Astron. Soc.* 400, 518 (2009).
32. M. Miyamoto and R. Nagai, *Publ. Astron. Soc. Jpn.* 27, 533 (1975).
33. L. Moscadelli, R. Cesaroni, M.J. Rioja, et al., *Astron. Astrophys.* 526, A66 (2011).
34. M.E. Popova and A.V. Loktin, *Astron. Lett.* 31, 663 (2005).
35. M.J. Reid, K.M. Menten, X.W. Zheng, et al., *Astrophys. J.* 700, 137 (2009a).
36. M.J. Reid, K.M. Menten, X.W. Zheng, et al., *Astrophys. J.* 705, 1548 (2009b).
37. M.J. Reid, J.E. McClintock, R. Narayan, et al., *Astrophys. J.* 742, 83 (2011).
38. K. Rohlfs, *Lectures on Density Wave Theory* (Springer, Berlin, 1977).
39. K.L.J. Rygl, A. Brunthaler, M.J. Reid, et al., *Astron. Astrophys.* 511, A2 (2010).
40. M. Sakai, M. Honma, H. Nakanishi, et al., *Publ. Astron. Soc. Jpn.* 64, 108 (2012).
41. R. Schönrich, *Mon. Not. R. Astron. Soc.* 427, 274 (2012).
42. R. Schönrich, J. Binney, and W. Dehnen, *Mon. Not. R. Astron. Soc.* 403, 1829 (2010).
43. A.S. Stepanishchev and V.V. Bobylev, *Astron. Lett.* 37, 254 (2011).
44. R.M. Torres, L. Loinard, A.J. Mioduszewski, et al., *Astrophys. J.* 671, 1813 (2007).
45. R.M. Torres, L. Loinard, A.J. Mioduszewski, et al., *Astrophys. J.* 698, 242 (2009).
46. Y.W. Wu, Y. Xu, K.M. Menten, et al., in *Cosmic Masers—from OH to H₀*, *Proceedings of the IAU Symposium No. 287*, Ed. by R.S. Booth, E.M.L. Humphreys, and W.H. T. Vlemmings (Cambridge, 2012), p. 425.
47. Y. Xu, J.J. Li, M.J. Reid, et al., *Astrophys. J.* 769, 15 (2013).
48. Y. Yamaguchi, T. Handa, T. Omodaka, et al., in *Proceedings of the East Asia VLBI Workshop 2012, May 30–Jun. 2, 2012* (2012).
49. M.V. Zabolotskikh, A.S. Rastorguev, and A.K. Dambis, *Astron. Lett.* 28, 454 (2002).
50. B. Zhang, M.J. Reid, K.M. Menten, et al., *Astron. Astrophys.* 544, A42 (2012).